RSC Advances

ROYAL SOCIETY OF CHEMISTRY

www.rsc.org/advances

Green fabrication of antibacterial polymer/silver nanoparticle nanohybrids by dual-spinneret electrospinning†

Runze Wang, [a,b] Zheng Wang, [a,b] Song Lin,* [a,b] Cheng Deng, [b] Fan Li, [b] Zhijian Chen*,[c] and Hua He [d]

a National Bio-Protection Engineering Center, Tianjin, People's Republic of China; Email: lynch163@163.com (S. Lin)

b Institute of Medical Equipment, Academy of Military Medical Sciences, Tianjin, People's Republic of China.

c School of Chemical Engineering and Technology, Tianjin University, Tianjin, People's Republic of China. Email: zjchen@tju.edu.cn (Z. Chen)

d Department of Neurosurgery, Changzheng Hospital, Second Affiliated Hospital of Second Military Medical University, Shanghai, People's Republic of China

†Electronic supplementary information (ESI) available: Additional SEM and TEM images.

Introduction

In the past decade, organic-inorganic hybrid nanomaterials have received tremendous attention owing to their widespread potential applications. [1, 2] As one of the important processing techniques to fabricate hybrid nanomaterials with multifunctional compositions, electrospinning is a highly versatile method that is capable of producing non-woven polymeric nanofibers with diameters ranging from a few nanometers to micrometers. The unique properties of such fibrous film have evoked significant interests in many fields. [3-5] A wide diversity of polymers have been successfully electrospun into ultrafine fibers with small pore and large surface-to-volume ratio which is very suitable for many biomedical and industrial applications, such as filtration, biological scaffolds, wound dressing materials and electrode materials.[6-12] In recent studies, the electrospinning of hybrid materials

consisting of two or more components, *i.e.* the incorporation of different polymers or metal nanoparticles (NPs) within the nanofibrous mats, has become one of the most promising and growing technologies today.[13-16] This multi-spinneret electrospinning method is relatively more simple and versatile to obtain hybrid materials with synergistic effects of individual component in order to improve the overall properties of the hybrid materials, such as strong antibacterial activity and favorable biocompatibility.[17-21]

Herein, we report a green and facile method to produce functional hybrid electrospun nanofibers with three-components: waterborne polyurethane (WPU), Poly (vinyl alcohol) (PVA) and silver nanoparticles (AgNPs). The development of WPU formulations has been motivated by environmental concerns as well as requirements of green chemistry. Waterborne polyurethane (WPU) is a superior material to traditional organic solvent-borne PU which not only inherits the merits of PU but also gets rid of the hazardous volatile organic compounds along with the benefit of low viscosity at high molecular weight, non-toxicity and non-flammable property.[20] However, the pure WPU dispersion cannot be directly electrospun because of low viscosity, which greatly limits its applications. One possible way is to introduce some kinds of hydrophilic and viscous polymers, i.e. poly (ethylene oxide) (PEO) [23] and poly (vinyl alcohol) (PVA), [24, 25] to serve as template polymers to produce WPU-containing nanofibers. On the other hand, PVA is a water-soluble polymer with fine biocompatibility, stability and water permeability, which make it to wide application in tissue regeneration, drug delivery and pharmaceuticals.[12]

In our previous work, [26] we have successfully prepared AgNPs-doped PVA nanofibers and evaluated their bioactive properties. Thus, in this study, we further report a dual-spinnerets method to electrospun 3-component hybrid nanofibrous mats composed of WPU/PVA/AgNPs. In the apparatus, two separate spinnerets were used to prevent gel formation or precipitation from direct mixing the solution of WPU and silver ions. In this green and facile procedure, water was used as the only solvent during the whole electrospinning process without addition of any other organic solvents. From the point of view of biomedical applications, such process is believed to be environmental friendly by completely avoiding the use of dimethylformamide (DMF) or tetrahydrofuran (THF) as solvents. In the meantime, the *in-situ* generation of ultrasmall AgNPs (ca. 5 nm) from silver nitrate ($AgNO_3$) was achieved in polyvinyl alcohol (PVA) aqueous solution via such a one-step methodology without any reductive chemicals. Herein, the abundant hydroxyl groups on the atactic PVA chains may act as both reducing agent and efficiently stabilizing agent for the fabrication of PVA/AgNPs composite nanofibers. Moreover, the PVA can serve as the electrospinning polymer matrix for AgNPs and WPU to obtain nanohybrid fibrous mats. After such hybrid fabrication, the as-prepared materials showed advanced performance in thermal stability as well as superior biocidal activity.[27] More interestingly, being low-toxic material, such 3-component WPU/PVA/AgNPs nanofibers designed in this paper may be a very promising candidate for application in biomedical areas.

Experimental Materials and Methods

Waterborne Polyurethane (WPU, UR301G, solid content = 30±2%, viscosity > 80 mPa·s) was obtained from Huanyu Polymers Co., Ltd, Wenzhou, People's Republic of China. PVA 1799 (99% alcoholysized, Mw =75,000) was purchased from Aladdin Industrial Co., Shanghai, People's Republic of China. $AgNO_3$ (99.8%) was purchased from Yingda Rare Chemical Reagents Factory, Tianjin, People's Republic of China. Nonwoven textile (50 $g \cdot m^{-2}$), made of polypropylene and polyethylene terephthalate fabrics, was obtained from Liyang New Material Development Co., Ltd, Nantong, People's Republic of China. Test bacteria such as Staphylococcus aureus (ATCC 6538) and Escherichia coli (8099) were purchased from the Institute of Microbiology and Epidemiology, Academy of Military Medical Science, People's Republic of China. Nutrient broth (NB) and agar powder were provided by Aoboxing Bio-tech Co., Ltd., Beijing, People's Republic of China. Electrospinning was carried out using a multinozzle electrospinning set-up system with movable (rotating and traversing) collector purposely built by our laboratory.

Preparation of nanofibrous mat of WPU/PVA (W-P)

Firstly 15% (w/v) PVA in deionized water was stirred in water-bath at 85°C for at least 2 hours to obtain the viscous solution as the batch solution. Then the WPU (UR301G) was firstly diluted to the solid content of 15% by deionized water. Different volume ratios, i.e. 3/7, 5/5, 7/3 of 15% PVA and WPU solutions were mixed and stirred for another 2 h at room temperature. Then it was pumped into a disposable syringe capped with an 18 gauge stainless steel cannula with a blunt end tip. During the electrospinning process, a high voltage (10kV or 15 kV or 20 kV) was applied to

the needle and solution was jetted at a flow rate of 1 $mL \cdot h^{-1}$ controlled by a syringe pump. A typical electrospinning process was as follows: the above mixed solution was poured into the plastic syringes and fixed on a syringe pump. Then a high voltage supply was connected with the steel needles of the syringes at the same time. The PVA/WPU solution was electrospun with the tip-to-collector distance (TD) of 15 cm. The nanofibers were collected on an aluminum drum covered by a piece of nonwoven textile fabrics as supporting material. After electrospinning, the obtained nanofibrous membrane was dried at room temperature and stored in a desiccator for further tests.

Dual-spinneret electrospinning of hybrid WPU/PVA/AgNPs (W-P-Ag)

To prepare the WPU/PVA nanofibers mats containing silver nanoparticles (WPU/PVA/AgNPs), two separate solutions were prepared in order to apply dual-spinneret method. Solution A is $AgNO_3$ in PVA aqueous solution, freshly prepared as reported elsewhere.[26] Briefly, 1% (w/v) $AgNO_3$ was dissolved in the solution of 12% (w/v) PVA, stirred vigorously for 0.5 h under dark at room temperature to obtain an isotropic solution, and then freshly used. Solution B is the WPU/PVA (3/7) aqueous solution as mentioned above. The two solutions are applied to the apparatus and electrospun at the same condition as previous experiment.

Thermal gravimetric analysis (TGA)

The thermal behavior of the as-prepared nanofibrous mats was studied with TGA /DSC 1 STAR^e system from Mettler Toledo, Switzerland at the rate of 10 ^oC/min from room temperature up to 600 ^oC under the nitrogen gas atmosphere (flow rate 20 mL/min).

TEM/SEM observation

The morphology of electrospun PVA nanofiber mats doped with AgNPs was observed with scanning electron microscopy (SEM) (FEI Nova Nano, SEM 230; FEI, Hillsboro, OR, USA) after gold coating under high vacuum (EMITECH K550x, Quorum Technologies Limited, East Grinstead, UK). The average diameter of the electrospun fibers was measured by Image-Pro Plus software (Media Cybernetics, Inc., Rockville, MD, USA) from the SEM images; and at least 50 counts of fibers from two separate images of each sample were measured. Energy dispersive X-ray spectroscopy (EDS) with accelerating voltage of 200 kV was measured from the SEM images. Elemental mapping was measured by high-angle annular dark-field scanning transmission electron microscopy/energy-dispersive spectrometry (HAADF-STEM /EDS). Transmission electron microscopy (TEM) analysis of the electrospun samples was conducted on Tecnai G2 F20 (FEI) equipped with electron diffractometer by using carbon Lacey film-coated copper grids (230 mesh, Beijing Zhongjing-keyi Technology Co., Ltd, People's Republic of China) as the supporter. The size of the AgNPs was measured using Image Pro Plus software from the TEM images (n=200). HRTEM images were taken in a JEOL JEM-2010FEF microscope operated at 200 kV.

X-ray photoelectron spectroscopy (XPS)

XPS was performed on the Thermo Scientific ESCALab 250Xi using 200 W monochromated Al Kα radiation. The 500 μm X-ray spot was used for XPS analysis. The base pressure in the analysis chamber was about 3×10^{-10} mbar. Typically the hydrocarbon C1s line at 284.8 eV from adventitious carbon is used for energy

referencing.

Inhibition zone assay

The antibacterial activity of composite nanofibers against both *S. aureus* (ATCC 6538) and *E.coli* (8099) were investigated by a zone inhibition method. Samples of nanofiber mats were cut into circular discs of 25 mm diameter. Using a spread plate method, nutrient agar plates were inoculated with 1 ml of bacterial suspension containing around 1×10^7 colony forming units (CFU)·mL^{-1} for each bacteria. Each sample was gently placed on the inoculated plates, and then incubated at 37^{o}C for 24 h. Zones of inhibition were observed and determined visually by measuring the clear area formed around each sample.

Cytotoxicity by cell counting kit-8 (CCK-8) assay

Each membrane, 10×20 mm, was incubated in 50 mL Dulbecco's Modified Eagle's Medium (DMEM) to obtain extract solution after 24 h of incubation with shaking in a 37°C humidified environment. Extracted solutions were filtered with 0.20 mm filter for sterilization and then diluted with fresh media to obtain different fractional concentrations, i.e., non-diluted [100%] and diluted extract solutions (1:7 [12.5%], 1:3 [25%], 1:1 [50%]) with DMEM, respectively. Fresh media without the extract solutions was designated as negative control (0%). Diluted and non-diluted extract solutions were then used to treat the PA317 cell line, 10^4 cells/mL, grown for 24 hours in the growth medium (DMEM with 10% fetal bovine serum [FBS]). Cell viability was quantified by CCK-8 kit following the protocol of the manufacturer (Dojindo Inc., Rockville, MD, USA).

Results and discussion

As depicted in Fig.1, electrospinning fabrication was carried out using a multinozzle electrospinning set-up system with movable aluminium collector purposely built by our laboratory. The collector can be rotating and traversing simultaneously in order to obtain uniform hybrid materials. Solution A is WPU/PVA and solution B is $AgNO_3$/PVA. By connecting with identical voltage of 15 kV, the designed 3-component hybrid WPU/PVA/AgNPs (W-P-Ag) nanofibrous mats can be obtained. (See experimental sections in ESI for details) For comparison, neat WPU/PVA nanofibers (W-P) were also prepared and examined by conventional single nozzle electrospinning. Figure 2 displays the SEM images of the as-prepared W-P nanofiber mats with different WPU/PVA charged ratios. At highest WPU/PVA ratio (7:3), many bead- and spindle-embedded fibers were formed (Figure 2a). Then the morphology was transformed to a spindle-like structure upon increasing content of PVA/WPU to 5:5 (Figure 2b). And finally the pure fibrous mats can be obtained at WPU/PVA ratio=7:3 (Figure 2c) because of highest viscosity of the solution. [28] Also, the diameters of the fibers become bigger as the viscosity increases (2^{nd} row in Fig. 2). Moreover, other parameters such as applied positive voltage and tip-to-collector distance (TD) during the electrospinning process were also investigated and the representative SEM images are shown in Fig. S1. By adjusting the positive voltage and TD, no distinct morphology was observed under the same WPU/PVA ratio. All the electrospun samples consist of randomly-oriented, ultrafine nanofibers with an average fiber diameter of 340 ± 50 nm，360 ± 45 nm，290 ± 35nm and 300 ± 35nm,

respectively, indicating the viscosity is the key factor in such system to obtain fibrous structures.

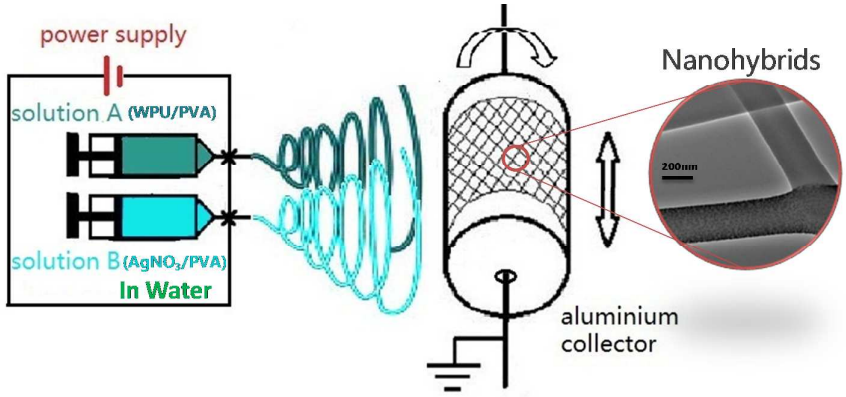

Figure 1 Schematic illustration of the designed setup of the two-spinneret electrospinning apparatus used in this study.

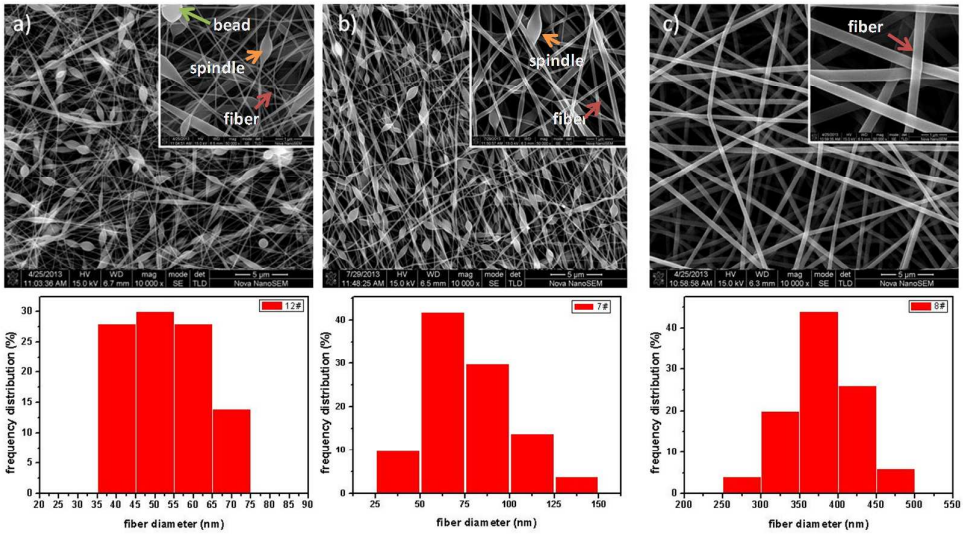

Figure 2. Typical SEM images of WPU/PVA nanofibrous mats at different WPU: PVA volume ratios: a) 7:3; b) 5:5; c) 3:7 @ Voltage = 15 kV and TD = 15 cm. The histograms on the second row below each image represents the statistic frequency distribution of obtained nanofibers with different diameters (50 counts), respectively. Scale bar: 5 μm and 1 μm (insets).

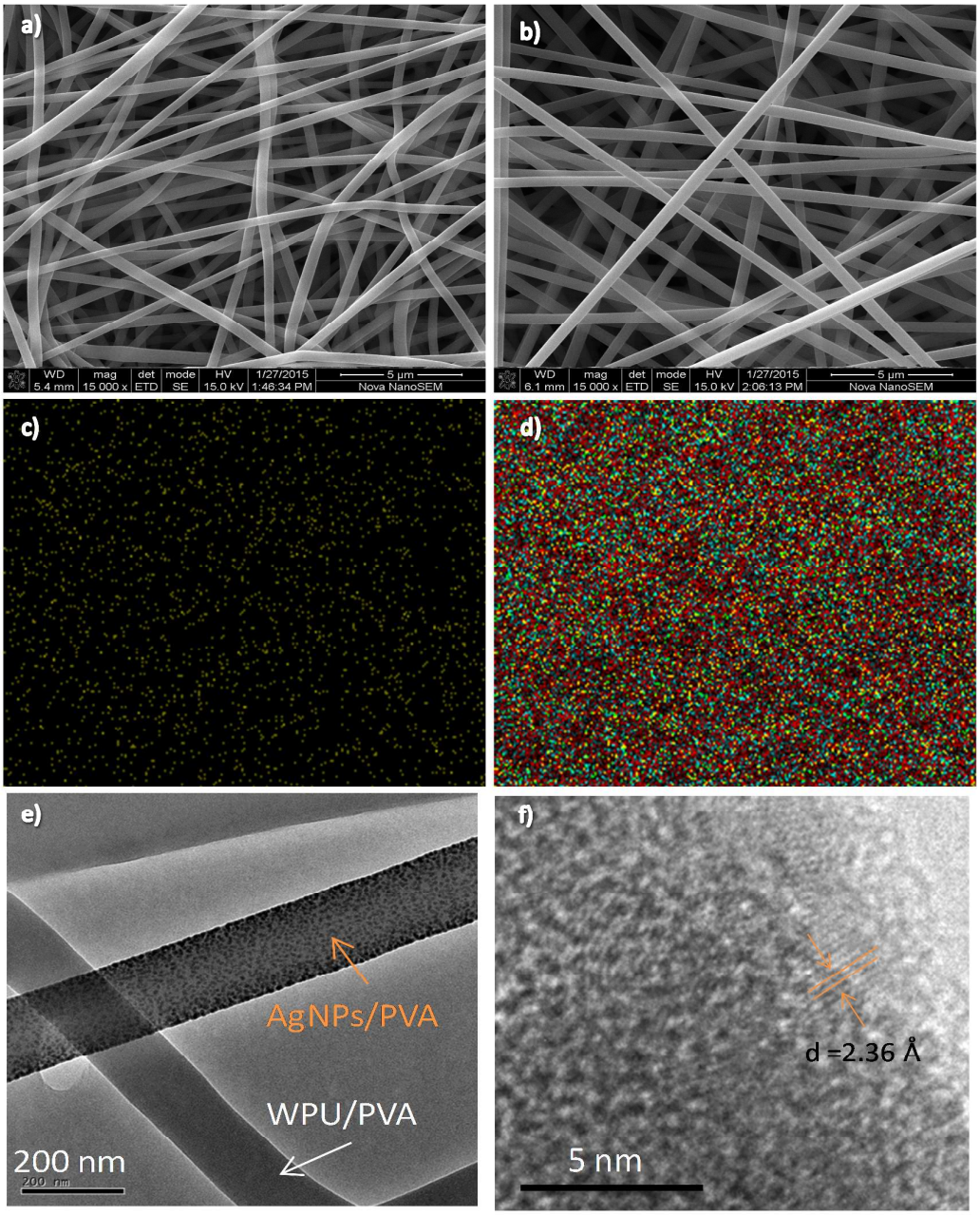

Figure 3. Typical SEM images of WPU/PVA (W-P, 3:7, a) and WPU/PVA/AgNPs (W-P-Ag, b) nanofibrous mats @ Voltage=15 kV and TD=15 cm. c) elemental distribution mapping of Ag in W-P-Ag as indicated by yellow pixels. d) the overlapped elemental distribution mapping of C (red), N (green), O (cyan) and Ag (yellow) in the sample W-P-Ag. e) TEM image of the as-prepared corresponding W-P-Ag sample. f) HRTEM image of AgNPs doped within PVA nanofibers (inter-plane spacing *d* is 2.36 Å)

After optimizing the W-P electrospun condition, the 3-component W-P-Ag was prepared under similar conditions. Under the SEM observation, both the samples of W-P (Figure 3a) and W-P-Ag (Figure 3b) show the same morphology with similar

diameters of fibers. However, in TEM images, the latter one clearly consist of two classes of nanofibers, *i.e.* AgNPs/PVA and WPU/PVA (Figure 3e), which indicates the successful preparation of hybrid 3-component W-P-Ag nanofibrous mats. In Figure 3f, a high resolution TEM image shows the lattice fringes with a *d*-spacing of 2.36 Å corresponding to the lattice spacing of the (111) planes of the Ag face-centered cubic (fcc) facet. [29, 30] Moreover, the size of obtained AgNPs doped in the PVA fibers under such condition is significantly small with size of ca. 5.1 ± 0.6 nm (Figure S2). The elemental mapping of the W-P-Ag nanofibers is shown in Figure 3c and 3d. It can be seen that the as-prepared AgNPs are uniformly distributed among the mats, indicating the WPU/PVA and PVA/AgNPs nanofibers are finely mixed. The PVA in such system is served as polymeric matrix to facilitate the formation of electrospun nanofibers with either WPU or AgNPs. Occasionally, some examples of merged and branched fibers can be observed as shown in Figure S3. Along with the evaporation of the solvent, the elongational flow from the two separated jet can meet and stick with each other, leading to the formation of the merged or branched hybrid fibers. [31]

Further X-ray photoelectron spectroscopy (XPS) studies (Figure 4) indicated that mere differences can be found in C1s and N1s peaks for the W-P and W-P-Ag samples. For the O1s peaks, two new peaks at 531.9 eV and 532.5 eV appeared after the *in-situ* formation of AgNPs in the W-P-Ag sample. This is assigned to the interaction between the hydroxyl groups along the PVA backbone and the Ag^{+} ions to produce AgNPs. [32] Most obviously, the doublet peaks in Ag_{3d} spectra at 368.2 eV and 374.2 eV are assigned to the binding energies $3d_{5/2}$ and $3d_{3/2}$, respectively, while for the W-P

sample, no such peaks were detected. (Fig. 4b)

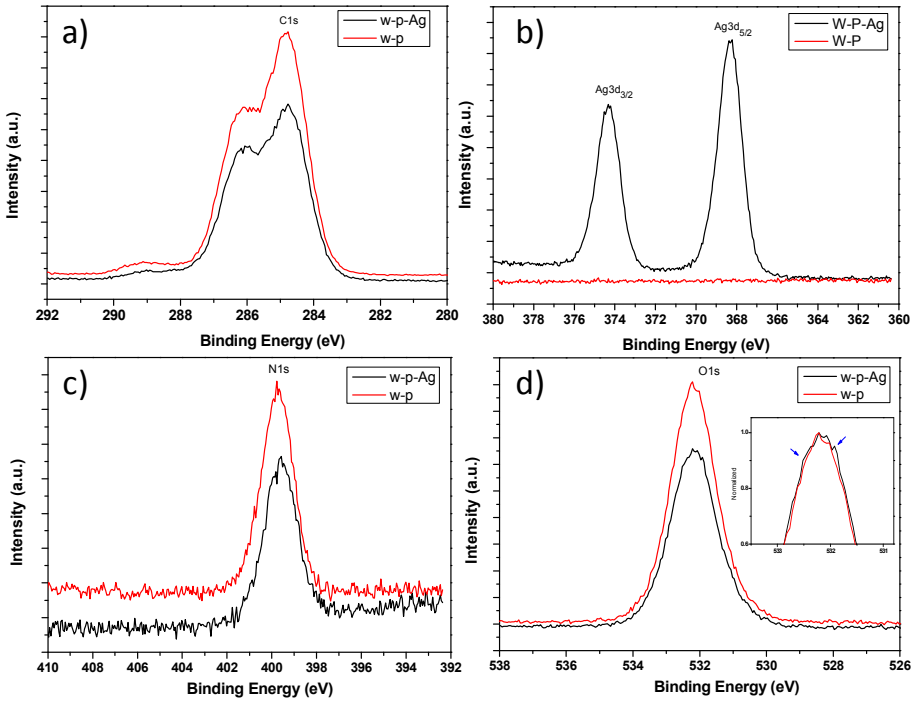

Figure 4. XPS spectra of C1s peaks (a), Ag_{3d} peaks (b), N1s peaks (c) and O1s peaks (d) in the samples of as-prepared W-P (red) and W-P-Ag (black) nanofibrous mats, respectively. The inset in (d) is the normalized O1s peak at an expanded scale.

The thermal stability of the as prepared hybrid nanocomposites was investigated by thermal gravimetric (TG) analysis (Fig. 5). The initial weight loss below 100 ^{o}C in all the samples could be attributed to removal of moisture content adsorbed on the surface or pores of the nanofibrous mats. For all the nanofiber mats, they show a similar two-step degradation process (step I and II) but with distinct degradation behavior. [33] In the case of pristine PVA polymer (control), the step-I, which ranges from 240 ^{o}C (onset point) to 320 ^{o}C (step I end point), shows a degradation of 68% weight loss. Then in step-II, a total decomposition of 82% in weight loss is observed while the temperature rises up to 500 ^{o}C (step II end point). In comparison, both WPU-containing samples, (W-P and W-P-Ag) show obviously improved thermal

stability, i.e. the hybrid 2-component WPU/PVA film shows an improvement in its thermal stability, with a decomposition of only 46% in a temperature range from 240^{o}C (onset point) to 350 ^{o}C (end point) in step I. In the case of WPU/PVA/AgNPs system, the TG curve matches very well with that of WPU/PVA system, indicating that the incorporation and presence of Ag nanoparticles have negligible impact on the thermal stability of the as-prepared film. The residual content is slightly higher in the WPU/PVA/AgNPs system due to the existence of Ag component. The final mass loss of both samples is above 90% when the temperature is up to 500 ^{o}C.

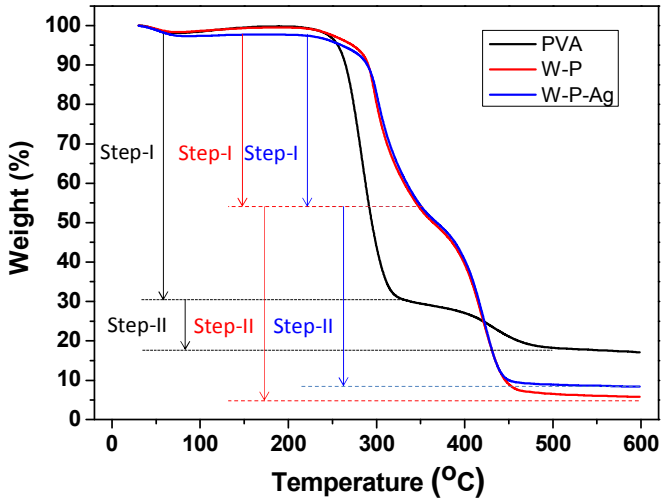

Figure 5. TG curves of the neat electrospun PVA polymer (black), WPU/PVA (5:5, red) and WPU/PVA/AgNPs (blue) hybrid nanocomposites. The corresponding colored arrows show the two steps (step-I and step-II) degradation progress of each nanocomposites, respectively.

The AgNPs-containing W-P-Ag nanofabrics herein also show excellent antibacterial activities. [34] The bacterial inhibition zone tests in Figure 6 show that all the AgNPs-containing samples have excellent inhibition activities against both *S. aureus* and *E. coli*. However, the AgNPs-free electrospun WPU/PVA sample (negative controls) did not show inhibition zones (Figure 6a &6c). A larger circular zone of

inhibition was observed against the S. *aureus test*, compared to the *E. coli* tests. As for the *S. aureus* tests, an approximate 2.4-fold increase in diameter of final inhibition zones compared to the initial diameter of W-P-Ag mats (Figure 6b). This is explained by the diffusion of AgNPs out of the fibrous mat, which killed bacteria within a certain diameter. However, for the *E. coli* tests, the diameter of the inhibition zone for the same sample is approximately 1.6-fold longer than the original one (Figure 6d). These results show that AgNPs in such system have a superior inhibition activity with *S. aureus*, compared to *E. coli*. The reason is believed to be the sophistication of the cell wall structures between gram-positive (*S. aureus*) and gram-negative (*E. coli*) bacteria. [35, 36]

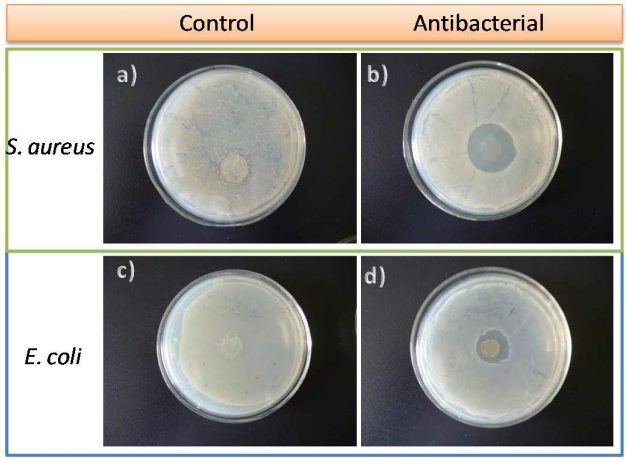

Figure 6. Zone of inhibition test against *S. aureus* (a&b) and *E. coli* (c&d) bacteria for nanofibrous mats, W-P (a & c) and W-P-Ag (b & d) as control and antibacterial materials, respectively.

Under inverted microscope observation (Fig. 7a and 7b), the PA317 cells treated with W-P as well as W-P-Ag nanofiber mats display normal morphology in both case, indicating that no obvious cytotoxic effect of the fibrous material towards the surrounding cells. Furthermore, the viability of the PA317 cells treated with W-P and W-P-Ag nanofibrous mats was evaluated using CCK-8 assay (Fig 7c). [37] As for the

W-P nanofibrous mat, the cell viability decreased from 88% to 84% with increase in the extract concentrations. Similar trends can also been found in the W-P-Ag sample. But the overall cytotoxicity of the two samples is low, since approximately 84% of cells remain alive when incubated with the non-diluted (100%) extract solutions. The existence of AgNPs shows no adverse effect in the cytotoxicity evaluation. This result is consistent with earlier results reported by our group [26] and others. [38]

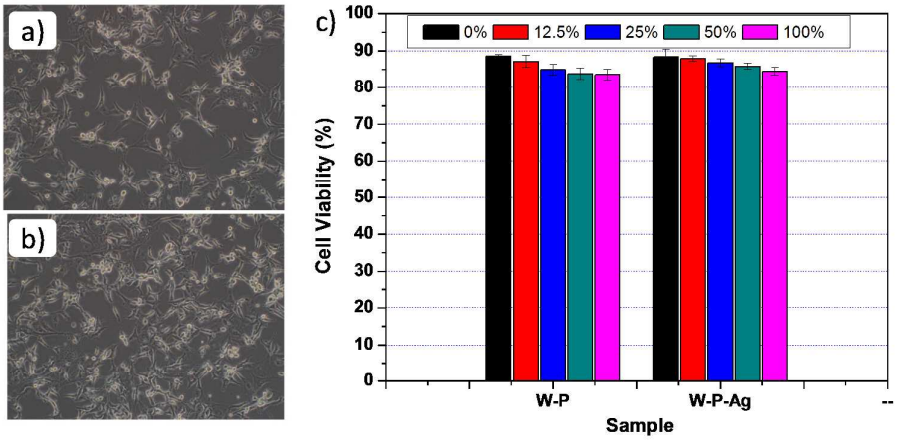

Figure 7. Optical micrograph of PA317 cells after the treatment with W-P (a) and W-P-Ag (b) nanofiber mats; (c) Cell viability of PA317 by CCK-8 assay with different concentrations of extract solutions of each sample (n=6)

Conclusion

The three-component WPU/PVA/AgNPs nanofiber mats were successfully electrospun from aqueous solution. The morphological studies indicated the nanofiber can be obtained by optimization of electrospinning parameters, such as applied voltage, tip-collector distance, viscosity of the solution and feed mass ratio. The electronic microscopic analysis indicates a uniform distribution of ultrasmall silver nanoparticles along the fibers. The elemental distribution mapping indicated the good mixture of WPU/PVA and PVA/AgNPs nanofibers in the mats via such dual-spinneret

technique. Also the thermal stability and biocidal activity of the W-P-Ag nanofibers were greatly enhanced by the addition of WPU component and incorporation of Ag nanoparticles without increase of cytotoxcicty. Moreover, the proposed fabrication method herein is cost-effective, eco-friendly and potential to be applied to functional materials with broad applications, such as antimicrobial agents, wound dressings, and water or air purification techniques.

Acknowledgements

We gratefully acknowledge the financial supports of the Project of National Natural Science Foundation of China (Grant No. 50903090, 21176184) and Tianjin Research Program of Applied Foundation and Advanced Technology (Grant No. 13JCQNJC02500).

Notes and References

[1] C. Sanchez, P. Belleville, M. Popall, and L. Nicole, *Chem. Soc. Rev.*, 2011, **40**, 696–753.
[2] X. Zhang, D. Gçrl, V. Stepanenko, and F. Wurthner, *Angew. Chemie Int. Ed.*, 2014, **53**, 1270–1274.
[3] Y. Si, J. Yu, X. Tang, J. Ge, and B. Ding, *Nat Commun*, 2014, **5**. doi:10.1038/ncomms6802
[4] C.-L. Zhang and S.-H. Yu, *Chem. Soc. Rev.*, 2014, **43**, 4423–4448.
[5] S. Hsu, K. Hung, Y.-Y. Lin, C. Su, H. Yeh, U. Jeng, C. Lu, S. A. Dai, W. Fu, and J. Lin, *J. Mater. Chem. B*, 2014, **2**, 5083–5092.
[6] Z. Huang, Y. Zhang, M. Kotaki, and S. Ramakrishna, *Compos. Sci. Technol.*, 2003, **63**, 2223–2253.
[7] D. Li and Y. Xia, *Adv. Mater.*, 2004, **16**, 1151–1170.
[8] R. Sahay, P. S. Kumar, R. Sridhar, J. Sundaramurthy, J. Venugopal, S. G. Mhaisalkar, and S. Ramakrishna, *J. Mater. Chem.*, 2012, **22**, 12953–12971.
[9] K. A. Rieger, N. P. Birch, and J. D. Schiffman, *J. Mater. Chem. B*, 2013, **1**, 4531–4541.
[10] F. E. Ahmed, B. S. Lalia, and R. Hashaikeh, *Desalination*, 2015, **356**, 15–30.
[11] V. Aravindan, J. Sundaramurthy, P. S. Kumar, Y.-S. Lee, S. Ramakrishna, and S. Madhavi, *Chem. Commun.*, 2015, **51**, 2225-2234.

[12] R. Sridhar, R. Lakshminarayanan, K. Madhaiyan, V. Amutha Barathi, K. H. C. Lim, and S. Ramakrishna, *Chem. Soc. Rev.*, 2015, **44**, 790–814.
[13] Y.J. Zhang, Y.D. Huang, L. Wang, F.F. Li, G.F. Gong, *Mater. Chem. Phys*., 2005, **91**, 217-222.
[14] A.E. Deniz, A. Celebioglu, F. Kayaci, T. Uyar, *Mater. Chem. Phys*., 2011, **129**, 701-704.
[15] S.K. Nataraj, B.H. Kim, M. dela Cruz, J. Ferraris, T.M. Aminabhavi, K.S. Yang, *Mater. Lett*., 2009, **63**, 218-220.
[16] L. D. Tijing, M. Tom, G. Ruelo, A. Amarjargal, H. Raj, C. Park, and C. Sang, *Mater. Chem. Phys.*, 2012, **134**, 557–561.
[17] S. Kidoaki, I.K. Kwon, T. Matsuda, *Biomaterials*, 2005, **26**, 37-46.
[18] M.Sun, X.H. Li, B.Ding, J.Y.Yu, G.Sun, *J. Colloid Interface Sci.*, 2010, **347**, 147-152.
[19] S. Honarbakhsh, B. Pourdeyhimi, *J. Mater. Sci*., 2011, **46**, 2874-2881.
[20]S. Changsarn, J.D. Mendez, K. Shanmuganathan, E.J. Foster, C. Weder, P. Supaphol, *Macromol. Rapid Commun*., 2011, **32**, 1367-1372.
[21] J. Han, J.F. Zhang, R.X. Yin, G.P. Ma, D.Z. Yang, J. Nie, *Carbohydr. Polym.*, 2011, **83**, 270-276.
[22] HC Kuan, CCM Ma, WP Chang, SM Yuen, HH Wu, TM Lee. *Compos Sci Technol* , 2005, **65**, 1703-1710.
[23] L. Buruaga, H. Sardon, L. Irusta, G. Alba, *Journal Of Applied Polymer Science*, 2009, **115**, 1176–1179.
[24] J. H. Yang, N. S. Yoon, J. H. Park, I. K. Kim, I. W. Cheong, Y. Deng, W. Oh, J. H. Yeum, *Journal of Applied Polymer Science*, 2011, **120**, 2337–2345.
[25]J. H. Park, I. K. Kim, J. Y. Choi, M. R. Karim, I. W. Cheong, W. Oh, and J. H. Yeum, *Polym. Polym. Compos.*, 2011, **19**, 753–7.
[26] S. Lin, R.-Z. Wang, Y. Yi, Z. Wang, L.-M. Hao, J.-H. Wu, G.-H. Hu, and H. He, *Int. J. Nanomedicine*, 2014, **9**, 3937–3947.
[27] Rai, M., Yadav, A., & Gade, A. *Biotechnology Advances,* 2009, **27**(1), 76–83
[28] H. Fong, I. Chun, and D. H. Reneker, *Polymer*, 1999, **40**, 4585–4592.
[29] A. Celebioglu, Z. Aytac, O. C. O. Umu, A. Dana, T. Tekinay, and T. Uyar, *Carbohydr. Polym.*, 2014, **99**, 808–816.
[30] T. Ghosh, P. Das, T. K. Chini, T. Ghosh, and B. Satpati, *Phys. Chem. Chem. Phys.*, 2014, **16**, 16730–16739.
[31] S.Koombhongse, W. Lin, D.H. Reneker. *J Polym Sci Part B: Polym Phys*, 2001, **39**, 2598-2606.
[32] N. Mahanta and S. Valiyaveettil, *RSC Adv.*, 2012, **2**, 11389–11396.
[33] S. Pandey, S. K. Pandey, V. Parashar, G. K. Mehrotra, and A. C. Pandey, *J. Mater. Chem.*, 2011, **21**, 17154–17159.
[34]F. Cheng, J. W. Betts, S. M. Kelly, J. Schaller, and T. Heinze, *Green Chem.*, 2013, **15**, 989–998.
[35] C. Z. Chen, N. C. Beck-Tan, P. Dhurjati, T. K. van Dyk, R. a LaRossa, and S. L. Cooper, *Biomacromolecules*, 2000, **1**, 473–480.
[36] S. Lin, J. Wu, H. Jia, L. Hao, R. Wang, and J. Qi, *RSC Adv.*, 2013, **3**,

20758–20764.
[37] W.Y. Zhou, B. Guo, M. Liu, R. Liao, ABM. Rabie, D. Jia. *J Biomed Mater Res*. 2010, **93,** 1574–1587.
[38] A. Panácek, M. Kolár, R. Vecerová, R. Prucek, J. Soukupová, V. Krystof, P. Hamal, R. Zboril, and L. Kvítek, *Biomaterials*, 2009, **30**, 6333–6340.